Journal of Theoretical Biology 264 (2010) 838–846

Contents lists available at ScienceDirect

Journal of Theoretical Biology

journal homepage: www.elsevier.com/locate/yjtbi

Receptor cross-talk in angiogenesis: Mapping environmental cues to cell phenotype using a stochastic, Boolean signaling network model

Amy L. Bauer [a,c,*], Trachette L. Jackson [b], Yi Jiang [a], Thimo Rohlf [c,d,1]

[a] Theoretical Division, Los Alamos National Laboratory, Los Alamos 87545, USA
[b] Department of Mathematics, University of Michigan, Ann Arbor 48109, USA
[c] Santa Fe Institute, 1399 Hyde Park Road, Santa Fe 87501, USA
[d] Max-Planck-Institute for Mathematics in the Sciences, Inselstr. 22, D-04103 Leipzig, Germany

ARTICLE INFO

Article history:
Received 14 July 2009
Received in revised form
24 January 2010
Accepted 16 March 2010
Available online 20 March 2010

Keywords:
Signal transduction
Integrin
Cadherin
Cancer
VEGF-RTK

ABSTRACT

Cancer invasion and metastasis depend on tumor-induced angiogenesis, the means by which cancer cells attract and maintain a blood supply. During angiogenesis, cellular processes are tightly coordinated by signaling molecules and their receptors. Understanding how endothelial cells synthesize multiple biochemical signals can catalyze the development of novel therapeutic strategies to combat cancer. This study is the first to propose a signal transduction model highlighting the cross-talk between key receptors involved in angiogenesis, namely the VEGF, integrin, and cadherin receptors. From experimental data, we construct a network model of receptor cross-talk and analyze its dynamics. We identify relationships between receptor activation combinations and cellular function, and show that cross-talk is crucial to phenotype determination. The network converges to a unique set of output states that correspond to known cell phenotypes: migratory, proliferating, quiescent, apoptotic, and it predicts one phenotype that challenges the "go or grow" hypothesis. Finally, we use the model to study protein inhibition and to suggest molecular targets for anti-angiogenic therapies.

1. Introduction

Endothelial cells are key constituents of the interior lining of all blood and lymphatic vessels, and are the targets of biochemical agents that stimulate cell growth and motility, thereby making them the key players in angiogenesis. Many growth factors and inhibitors have been discovered to regulate angiogenesis (e.g., Folkman, 2006). Amongst those $VEGF_A$ plays a major role in regulating endothelial cell migration, proliferation, and survival (Gerhardt et al., 2003). However, it is not at all clear how cells interpret the $VEGF_A$ signal in the context of other signals and decide which cellular phenotype to adopt. Previous studies have targeted VEGF co-receptors flt-1 (Yancopoulos et al., 2000) and neuropilin (Ferrara et al., 2003) in an attempt to explain the different phenotype expressions, but a comprehensive picture remains elusive. During angiogenesis, the VEGF growth factor receptor tyrosine kinase (RTK), integrin (ITG), and cadherin signaling pathways are highly connected and provide regulatory feedback to each other (Gagne et al., 2004; Somanath et al., 2009), a process referred to as receptor cross-talk. As examples, in response to VEGF, endothelial cells upregulate the expression of integrin receptors (Mantzaris et al., 2004; Somanath et al., 2009) and Hutchings et al. (2003) found that integrins can additionally serve as receptors for immobilized $VEGF_{165}$ and $VEGF_{189}$ present in the extracellular matrix (ECM). Through growth factor receptors, VEGF activates the MAPK signal transduction pathway stimulating proliferation and cell survival. Cell survival and proliferation, however, critically depend on adherence to the ECM, since even in the presence of stimulating concentrations of growth factor, loss of anchorage to the ECM results in cell cycle cessation and apoptosis (Chen et al., 1998; Huang and Ingber, 1999). Another example of receptor cross-talk in angiogenesis occurs through cadherin activation. Cadherins induce signals that mitigate growth factor activation and repress cell proliferation (Zanetti et al., 2002) in a process termed contact inhibition (Gottardi et al., 2001). Thus cadherin receptors facilitate cell–cell communication and mediate proliferation. Cells naturally integrate concurrent signals from growth factor, integrin, and cadherin receptors to determine cell phenotype and dynamically regulate angiogenic processes (Sephel et al., 1996). This study is the first to propose a signal transduction network model that couples VEGF–RTK, ITG, and cadherin receptor signaling cascades, key receptors activated during angiogenesis, to capture receptor

* Correspondence to: Theoretical Division, Mail Stop B262, Los Alamos National Laboratory, Los Alamos 87544, USA. Tel.: +1 505 665 0416; fax: +1 505 665 4063.
E-mail addresses: albauer@lanl.gov, albaeur@umich.edu (A.L. Bauer).
[1] Present address: Programme d'Epigenomique, Tour Evry 2, 523 Terrasses de l'Agora, F-91034 Evry, France. Bastolla, U., Parisi, G., 1998. The modular structure of Kauffman networks. Physica D 115, 219–233.

0022-5193/$ - see front matter © 2010 Elsevier Ltd. All rights reserved.
doi:10.1016/j.jtbi.2010.03.025

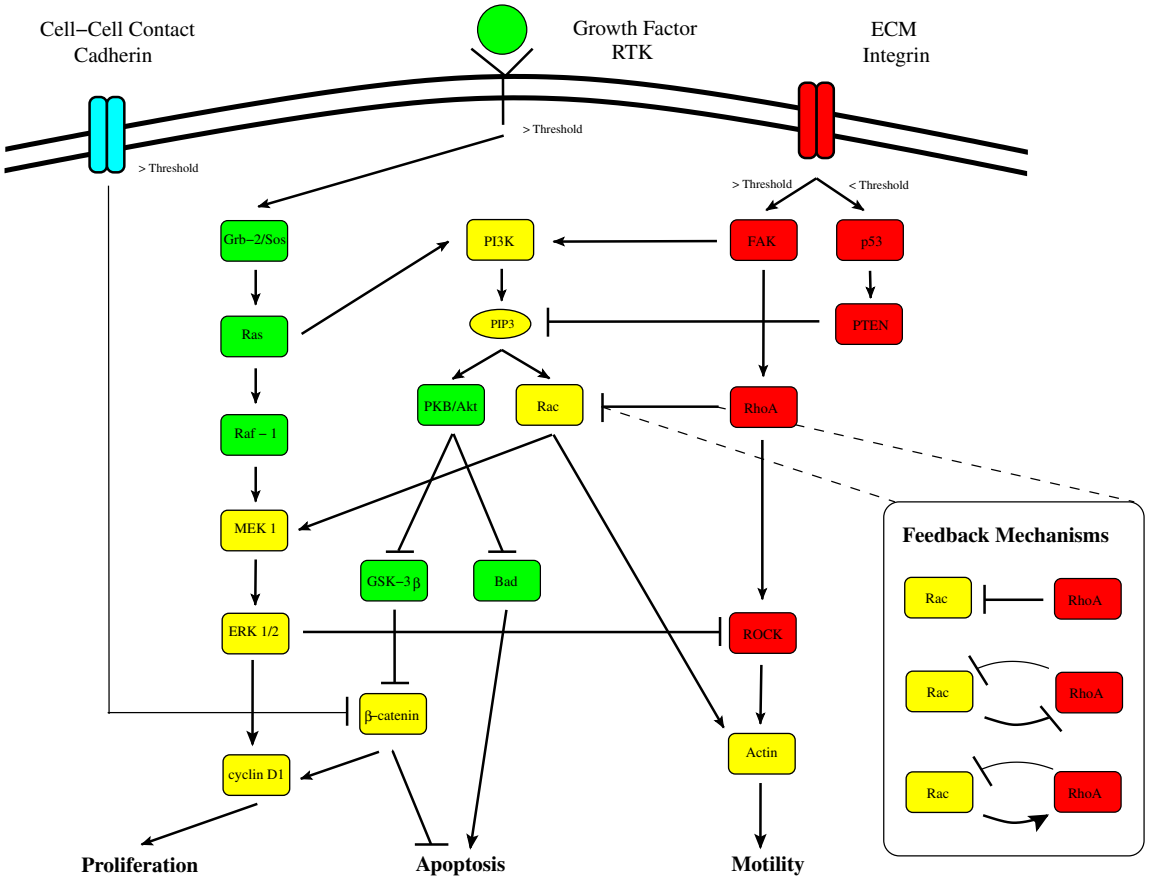

Fig. 1. Model of receptor crosstalk during angiogenesis. Reduced signal transduction network linking external stimuli to a cell's internal decision making machinery and cell phenotype. This network highlights the relationships between growth factor, integrin, and cadherin receptors, allowing for cross-talk between the three to ultimately decide the cell's fate. Colors associate downstream molecules with the initiating receptor: green denotes the VEGF–RTK pathway, red the ITG pathway, blue the cadherin, and yellow identifies molecules influenced by multiple receptors (cross-talk). An arrow between nodes signifies activation and a hammerhead indicates an inhibitory effect. Inset: different feedback scenarios between Rac1 and RhoA supported by experimental evidence. (For interpretation of the references to color in this figure legend, the reader is referred to the web version of this article.)

cross-talk during angiogenesis. We use this model to investigate how cellular behavior depends on and is controlled by changing environmental signals. We explain the regulation of critical cellular phenotypes based on receptor cross-talk and how this information can be used to devise new pro- and anti-angiogenic therapies for treating cancer and other angiogenesis-dependent diseases.

2. Model development

Driven by the scarcity of quantitative kinetic data for the biochemical reactions of interest, we develop a stochastic Boolean network model to describe the signal transduction pathways critical to cellular regulation and function during angiogenesis. Fig. 1 graphically represents the signal transduction network we implement for this study. This network characterizes the key signaling pathways activated during angiogenesis. An arrow between nodes signifies activation and a hammerhead indicates an inhibitory effect. This signaling network synthesizes the empirical data available for endothelial cell signal transduction during critical angiogenic processes using the sparsest graph consistent with all experimental observations. We integrate data from signaling databases (KEGG; STKE) with results from experiments to determine the dependence relation for each signaling molecule in the network (Table 1). From this starting point, we first develop a standard discrete Boolean network (BN) that treats molecular species as binary (on or off) Boolean variables $X_i(t)$, i.e., they are either present or absent depending on the state of other molecular species. Each species i has k_i regulators, $r_i^1,\ldots,r_i^{k_i}$ and a Boolean regulation function $f_i:[0,1]^{k_i}\to[0,1]$. The dependence relation for each species is given in Table 1. The state of species i at time $t+1$ then is given by

$$X_i(t+1)=f_i(X_{r_i}^1(t),\ldots,X_{r_i}^{k_i}(t)). \quad (1)$$

Boolean networks with randomly assigned interactions and update rules were originally proposed as simplified models of large gene regulatory networks (Kauffman, 1969; Thomas, 1973). Despite its simple deterministic update rules, this model exhibits rich dynamical behavior. In particular, BNs exhibit an order–disorder phase transition when each unit has on average two inputs from other nodes. Combinatorial and statistical methods have provided detailed knowledge about properties of BNs near the critical point (Derrida and Pomeau, 1986; Solé and Luque, 1995; Kaufman et al., 2005; Rohlf, 2008a; Bastolla and Parisi, 1998). BNs have been applied as abstract models for the adaptive evolution of gene regulatory networks (Bornholdt and Sneppen, 1998; Bornholdt and Rohlf, 2000; Rohlf, 2008b), as well as for the study of particular biological problems, e.g., pattern formation and morphogenesis in multi-cellular animals (Albert and Othmer, 2003; Rohlf and Bornholdt, 2009), stability of the yeast cell cycle (Li et al., 2004) and signal transduction in plants (Song Li and

Table 1
Table of Boolean network interactions. Table summarizing the Boolean dependence relation for each node in Fig. 1 determined based on experimental data. For instance, Ras is activated if Grb-2 is, whereas GSK-3β is inhibited when Akt is activated. Most of this information is specific to endothelial cells, but data from other cells lines are included where information on the endothelial cell line is lacking.

Node	Dependence relation	Reference
Cadherin	External signal (cadherin) binding)	Zanetti et al. (2002)
VEGF–RTK	External signal (RTK)	Ferrara et al. (2003)
ITG	External signal (integrin) binding)	Ruoslahti and Reed (1994)
Grb-2/Sos	VEGF-RTK	Ferrara et al. (2003)
Ras	Grb-2/Sos	Zanetti et al. (2002)
Raf-1	Ras	Cox and Der (2003)
MEK 1	Raf-1 OR Rac1	Eblen et al. (2002)
ERK 1/2	MEK 1	Cox and Der (2003)
PI3K	Ras AND FAK	Ruoslahti and Reed (1994), Cox and Der (2003), Datta et al. (1999)
PIP3	PI3 K AND NOT PTEN	Leevers et al. (1999), Okumura et al. (1996)
PKB/Akt	PIP3	Datta et al. (1999)
Rac1[a]	PIP3 AND NOT RhoA (inactive)	Nobes and Hall (1995), Leevers et al. (1999), Schoenwaelder and Burridge (1999)
GSK-3β	NOT PKB/Akt	Datta et al. (1999)
Bad	NOT PKB/Akt	Cox and Der (2003)
β-catenin	NOT cadherin AND NOT GSK-3β	Rubinfeld et al. (1996), Gottardi et al. (2001), Lampugnani et al. (2003)
FAK	ITG	Abedi and Zachary (1995)
p53	NOT ITG	Ishizaki et al. (1997)
PTEN	p53	Stromblad et al. (1996)
RhoA	FAK	KEGG
ROCK	RhoA AND NOT ERK 1/2	Ishizaki et al. (1997)
Actin	ROCK OR Rac1	Amano et al. (1996), Keely et al. (1997)
cyclin D1	ERK 1/2 AND β-catenin	Gottardi et al. (2001)
Proliferation	cyclin D1	Lampugnani et al. (2003)
Apoptosis	Bad AND NOT β-catenin	Datta et al. (1999)
Motility	Actin	Pollard and Borisy (2003)

[a] OR NOT if activated.

Albert, 2006). Interestingly, the problem that we address in this paper is rooted in two of the above-mentioned applications, synthesizing questions from both signal transduction and morphogenesis at the cellular level.

It has long been recognized that standard BN with their deterministic, discrete dynamics and synchronous, clock-wise updates represent a major oversimplification of real regulatory networks. Real network dynamics is noisy and asynchronous, and is based on smooth transitions of molecular switches. Continuous time switching networks were introduced as a differential equation model of gene expression dynamics to overcome some of these limitations of standard BNs (Glass, 1973, 1975). Glass' model is more realistic in that it allows for asynchronous switching and smooth transitions, however, it still neglects noise in molecular interactions. Here we present a novel Glass-type stochastic model of signal transduction. Each molecular species, i, has a real-valued, normalized concentration level as a function of time, denoted $x_i(t)\in[0,1]$. Based on this concentration level, each molecular species is associated with a binary (on or off) Boolean state $X_i(t)$ via a threshold switching mechanism

$$X_i(t)=\begin{cases}1, & \text{if } x_i\ (t)\geq 1/2\\ 0, & \text{if } x_i\ (t)<1/2.\end{cases}$$

As in the case of discrete, standard Boolean networks defined in Eq. (1), each species i has k_i regulators, $r_i^1,\ldots,r_i^{k_i}$ and a Boolean regulation function $f_i:[0,1]^{k_i}\to[0,1]$. The continuous time dynamics of species i is given by the following stochastic differential equation:

$$\frac{dx_i(t)}{dt}=|f_i(X_{r_i}^1(t),\ldots,X_{r_i}^{k_i}(t))-\delta(t)|-x_i(t). \tag{2}$$

Notice that Eq. (2) has the form of a production-decay differential equation, hence $f_i(t)$ is referred to as the production rate of molecular species i at time t, and $f_i(t)$ plays the role of a production rate function. Since concentrations of signaling molecules in cells are usually relatively low, one can expect that a substantial amount of noise (randomness) occurs in molecular interactions. To account for this, we introduce the stochastic variable $\delta(t)$ in Eq. (1), such that

$$\delta(t)=\begin{cases}1, & \text{with probability } p\\ 0, & \text{with probability } 1-p,\end{cases}$$

where $p\in[0,1/2]$. Notice that for $p=0$, the dynamics are completely deterministic, whereas $p=1/2$ corresponds to a complete randomization of the production rate function, i.e., making it a random switch. In between, $0<p<1/2$, the Boolean update executes with an error rate p, since when $\delta(t)=1$, the output determined by $f_i(t)$ is always inverted. Initially, internal network nodes are set to randomly chosen concentration levels drawn from a uniform distribution in [0,1]. From this starting state, dynamics are iterated for all network elements according to Eq. (2), while external signals are held constant.

Let us briefly comment on the relationship between the stochastic, continuous-time system defined by Eq. (2) and the deterministic, discrete time system of standard Boolean networks, as defined in Eq. (1). If we replace the differentials in Eq. (2) with finite differences Δx_i and Δt, it follows that:

$$x_i(t+1)=x_i(t)+\Delta x_i=x_i(t)+[|f_i(X_i^1,\ldots,X_i^{k_i})-\delta(t)|-x_i(t)]\Delta t. \tag{3}$$

Evidently, for $\Delta t=1$ and $p=0$ this reduces to Eq. (1), i.e., to a standard deterministic Boolean network with discrete time and discrete states. For $\Delta t=1$ and $p>0$, the system transforms into a Boolean network that performs updates of the binary states with error rate p, providing direct correspondence to other recent studies concerned with the effect of similar update noise in the nodes of discrete time Boolean networks (Peixoto and Drossel, 2009). Other types of noise, e.g., delays in signal transmission (Klemm and Bornholdt, 2005) are not considered in this work.

3. Results and discussion

3.1. Cellular behavior and angiogenic control explained by stochastic network model of receptor cross-talk

Based on the experimental data published in the literature, we construct a signal transduction network that includes VEGF–RTK, integrin, and cadherin receptor signaling pathways and their cross-talk (Fig. 1). Using this network, we systematically test all possible receptor activation combinations, with the internal network nodes initially set to randomly chosen binary states (discrete Boolean model) or to randomly chosen molecular concentrations (continuous time model). We find that, independent of the initial state of the internal nodes, the network converges to a unique set of output states that correspond to known cell phenotypes: migratory, proliferating, quiescent, apoptotic, and predicts one phenotype that contradicts the "go or grow" hypothesis, in which the cell is both migrating and proliferating. Fig. 2 shows the time evolution of the discrete Boolean network for three examples of external input configurations. The initial states of all internal nodes are set to 0. The network dynamics quickly converges to unique fixed points, and correspondingly, well-defined output states that depend only on the combinations of VEGF–RTK, integrin, and cadherin receptor states. Robustness of the dynamics against fluctuations in initial internal states is verified by a systematic enumeration of all possible 2^19=524288 initial combinations of 1s and 0s in internal nodes states. In all cases, the final output state depends only on the external inputs, with only a slight increase of convergence time compared to the dynamics with initial states of internal nodes all set to 0. These results are also confirmed using the continuous-time dynamics of Eq. (2) with moderate noise levels and fluctuations in initial internal concentrations. Hence, we have verified that the final, stationary state of network dynamics depends only on the external inputs provided.

This systematic investigation of the possible input combinations and the resulting fixed points of network dynamics allow us to construct an input–output map that uniquely characterizes cellular response to external stimuli with regard to cellular phenotype. Fig. 3 shows this predicted mapping between receptor activation state and cellular behavior for the baseline network. Colors distinguish the different phenotypes: apoptotic, proliferating, migrating, quiescent, and both proliferating and migrating and are represented by gray, green, red, white, and bi-colored, respectively. Consistent with experimental observation, the absence of either growth factor or integrin receptor activation always induces apoptosis (gray) (Hutchings et al., 2003; Ruoslahti and Reed, 1994). When signals for both growth (VEGF–RTK) and motility (ITG) are present, cross-talk plays a crucial role in determining the actual phenotype of the cell. This can be seen from the effect of activating or deactivating Rac1, a central player mediating cross-talk in this network. Referring again to Fig. 3, for contact inhibited cells (bottom two rows), activation of Rac1 produces a cell phenotype that is motile, but not proliferating, while, interestingly, deactivating Rac1 produces quiescent cells. The prediction of a quiescent cell type was surprising and encouraging as it is an emergent, rather than engineered, property of the network. On the other hand, in the absence of contact inhibition, deactivation of Rac1 shunts cell growth, whereas when Rac1 is active, the cell exhibits both growth and motility. This latter finding contradicts the widely believed "go or grow" hypothesis, which proposes that cell division and cell migration are temporally exclusive events. In support of our

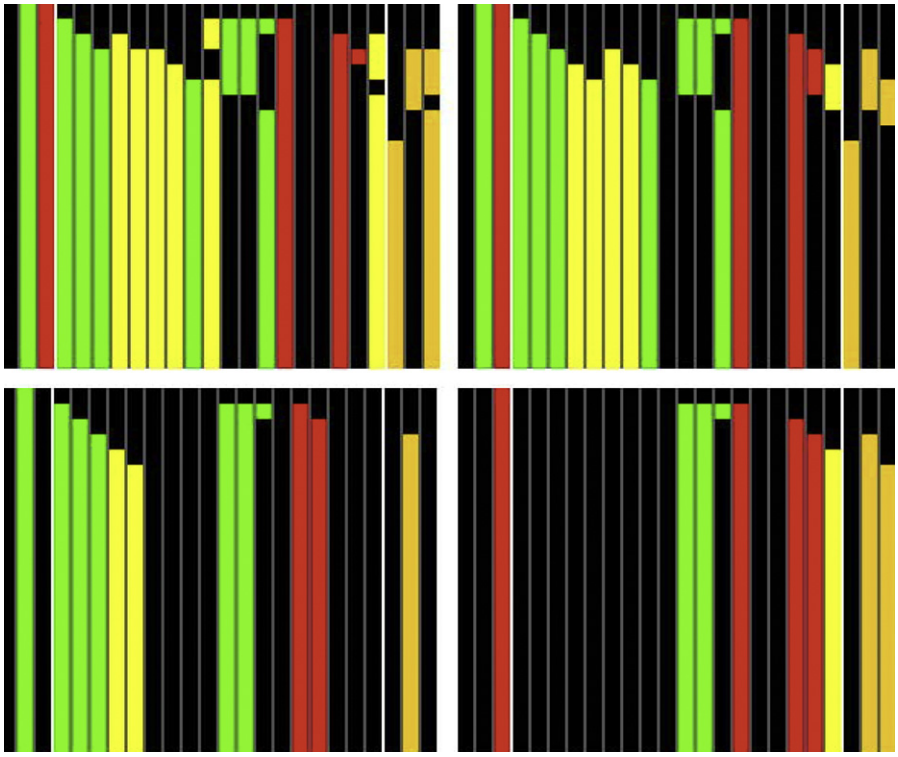

Fig. 2. Space-time plots of the dynamics of the discrete Boolean network. External inputs leftmost (cadherin, VEGF–RTK, ITG) and outputs on far right in orange (from left to right: proliferation, apoptosis, motility); time runs from top to bottom. Colors correspond to the molecular nodes in Fig. 1, with black cells indicating that the corresponding node has state 0. Upper panels: external signals cadherin and VEGF-RTK present, no contact inhibition leads to "go and grow phenotype"; Rac1 activated (left); the same with deactivated Rac1 (right). Lower panels: cadherin input only (left) as well as VEGF-RTK input only lead to apoptosis (Rac1 active). (For interpretation of the references to color in this figure legend, the reader is referred to the web version of this article.)

finding, an experiment using human medulloblastoma cancer cells has produced evidence contrary to the "go or grow" dogma (Corcoran and Del Maestro, 2003). In addition, very recent 4D (x,y,z,t) imaging results of developing quail embryos in vivo were used to generate plots of endothelial cell cycle and cell motility in time that reveal coincident migration and proliferation (personal communication with Dr. Russell Lansford, manuscript submitted). Understanding that cells can migrate while they prepare for division is a fundamentally different perspective from traditional interpretations of experimental results and treatment of cellular behavior in mathematical models of angiogenesis. For cancer cells, whose primary goal it is to grow and invade, it is easy to grasp that there is efficiency in coordinating cellular functions, especially in the most invasive and rapidly growing cell lines, such as glioblastoma cells. Endothelial cells have essentially the same goal when stimulated by tumor-secreted growth factors. Thus, it should not be surprising that endothelial cells may also exhibit growth coincident with migration. It should be noted, however, that motile cells stop migrating in M phase, but that constitutes only a small fraction of the whole growth cycle. In a new vessel sprout, endothelial cells are typically classified as tip cells and stalk cells. Tip cells are phenotypically different than their stalk cell counterparts, distinguished by their extraordinary motile ability, high expression of VEGF receptors, and presence of filopodia (Gerhardt et al., 2003). We find, in our simulations of sprout formation, that sprout tips consist of cells with the "go *and* grow" phenotype (Bauer, 2007), suggesting the possibility that the tip cell phenotype is the same as the "go *and* grow" phenotype. This hypothesis can be experimentally verified. Labeling cells for proteins specific to proliferation and migration in time-lapse studies will provide further insight. If the hypothesis that the tip cell phenotype coincides with the "go *and* grow" phenotype is true, then regulating the "go *and* grow" phenotype, by manipulating the signaling network, either through signaling molecules, cell surface receptors, or the network topology, would promise to have pro- or anti-angiogenesis effects.

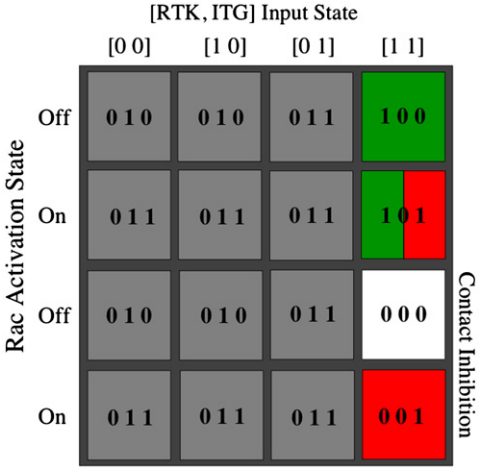

Fig. 3. Network predicts cell phenotypes as a function of external signals. Grid summarizing cell phenotype predictions by the Boolean network for various input configurations, where, for example, [10] denotes a VEGF–RTK signal only and output (100) indicates proliferation. This Boolean network model exhibits five critical and distinct cell phenotypes: apoptotic, proliferating, migrating, quiescent, and both proliferating and migrating (respectively gray, green, red, white, bicolor). (For interpretation of the references to color in this figure legend, the reader is referred to the web version of this article.)

3.2. Network performance is robust

We conduct several studies to gauge the robustness of the network's performance. Fig. 4 shows the response of the network to a sudden change in external stimulus, in this case the loss of the integrin signal (white arrow). Before ITG signal loss, the cell exhibits a "go and grow" response. Once the loss of signal propagates through the network, an apoptotic response ensues (red arrow). While the system is very sensitive to external signals, it is also very robust against fluctuations in concentrations. We test this by varying the level of noise p in the production rate function between 0 and its maximum 0.5. We find that the network response (phenotype map), as shown in Fig. 3, is reliably produced (100%) when we introduce error rates of up to 35% in Boolean function execution. Above a 35% error rate, the phenotypes predicted in Fig. 3 are still predominantly produced, however, larger error rates can generate phenotypes that deviate from this mapping. For example, oscillations arise in the output signal, or, apoptosis instead of migration is predicted.

To further quantify the robustness of the signaling network dynamics, we also study the average phenotype error rate e_p (averaged over all network outputs) as a function of system noise p, for different time step sizes dt (see Eq. (2)). Decreasing dt is equivalent to increasing the concentrations of molecules needed for signal amplification, that is, it represents a smoothing of the response curve (conversely, as previously mentioned, letting dt go

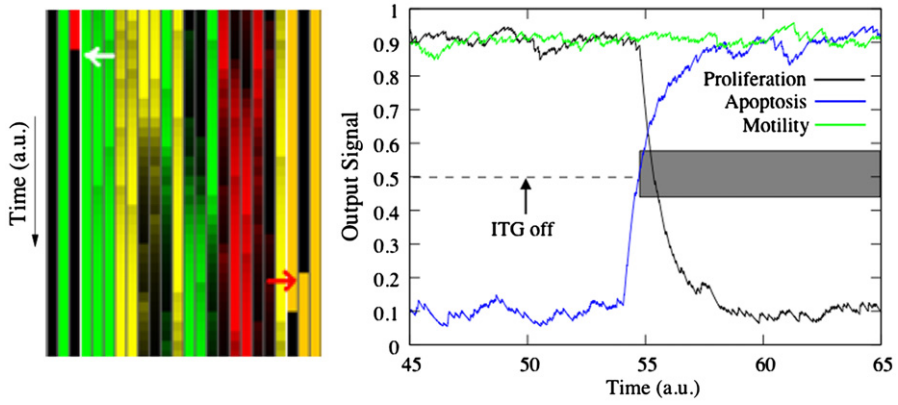

Fig. 4. Robust and rapid network response. Left: Screenshot of system dynamics (continous time Boolean network with noise level $p=0.1$). External inputs are leftmost (cadherin, VEGF–RTK, ITG) and outputs on far right in orange; time runs from top to bottom. Colors correspond to the molecular nodes in Fig. 1. White arrow indicates where the ITG signal is turned off; red arrow indicates the resulting change in phenotype response (from "go & grow" to apoptosis). Right: Output response (real valued concentration level) as a function of time. Blocking the ITG receptor signal induces an apoptotic response. Results are obtained using a noise level $p=0.1$. (For interpretation of the references to color in this figure legend, the reader is referred to the web version of this article.)

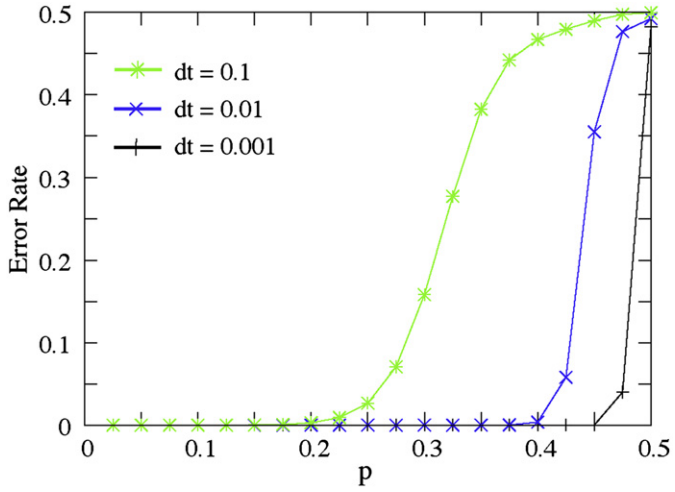

Fig. 5. Network is robust to noise in internal signals. Average phenotype error rate (i.e. fraction of "wrong" output states) averaged over 10,000 iterations of the discretized set of differential equations (Eq. 1), for three different time step sizes ($dt=0.1$, $dt=0.01$, $dt=0.001$). Decreasing dt is equivalent to increasing the average concentration of signaling molecules. For all $dt<1$, there is a sharp transition at a finite value p_c of the error rate e_p, below which phenotype errors vanish.

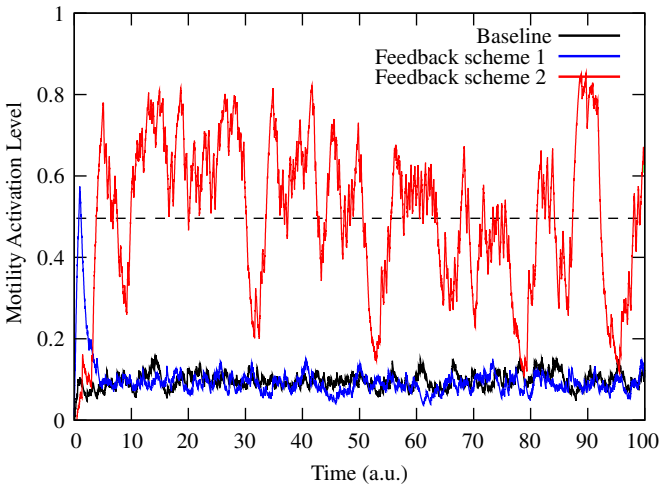

Fig. 6. Positive Rac1/RhoA feedback loop predicted. Motility response given VEGF–RTK and ITG signals with low Rac1 activity at a noise rate $p=0.1$. Both the baseline network and the network where RhoA and Rac1 inhibit each other (feedback scheme 1) lead to proper regulation and inhibit motility (signal well below 0.5). If Rac1 activates RhoA (feedback scheme 2), even low levels of noise lead to an erratic output signal with strong fluctuations around 0.5, and hence an erratic on–off pattern of motility. Since this type of cellular behavior is dysfunctional, we postulate that, with high probability, feedback scheme 2 is ***not*** realized in normal, healthy cells in this biological system. This finding suggests that manipulation of the Rac1/RhoA feedback loop may induce anti-angiogenic effects.

to 1 corresponds to a complete discretization). Fig. 5 summarizes the findings. For all $dt<1$, there is always a finite value p_c below which phenotype errors e_p vanish. For example, when $dt=0.1$, $p_c=0.2$. This indicates a high robustness of signal transduction against molecular noise, even at very low molecular concentrations as is typically found in living cells. For different values of dt, e_p is between 0 and an upper bound 0.5. As shown in Fig. 4, decreasing dt shifts the p_c transition towards $p=0.5$.

3.3. Study of Rac1 and RhoA interactions predicts conditions leading to erratic cell motion suggesting most viable feedback mechanism for successful angiogenesis

We have shown that this mathematical model of VEGF–RTK–ITG–cadherin receptor cross-talk captures the known cellular phenotypes and that signal transduction is robust against concentration fluctuations and molecular noise. Since Rac1 and RhoA are principal players in cross-talk between integrin and growth signals, we use this model to investigate the effects of various reported feedback schemes on system dynamics and cellular phenotype. A number of experimental studies focus on the interplay between these molecules (e.g., Yancopoulos et al., 2000; Ferrara et al., 2003; Nobes and Hall, 1995; Abedi and Zachary, 1995). The inset in Fig. 1 shows three different interaction schemes that are discussed in the literature. Using our network model, we compare these three possible relationships between RhoA and Rac1 and show which combinations of Rac1 (de)activation and cadherin regulated contact inhibition control cell quiescence, growth, apoptosis, and motility (Fig. 3). We find that simulations using either the baseline circuit (bl) without Rac1 feedback or the positive feedback circuit (fb1) lead to stationary dynamics that are highly robust against noise. Both bl and fb1 suppress the signal for motility. Interestingly, a mixed feedback scheme (fb2), in which Rac1 activates RhoA and RhoA inhibits Rac1, is extremely sensitive to noise, while, for zero noise, it behaves as a highly regular oscillator. The resulting cellular phenotype for fb2, given growth factor and integrin signals with low Rac1 activity, is an erratic, dysfunctional on–off pattern of cell motility (Fig. 6). This is true even for very low levels of noise, indicating a complete breakdown of motility regulation. Since robustness against fluctuations of molecular concentrations is a key requirement for living cells, we predict, with a high probability, that to suppress these strong nonlinear effects, either feedback circuit fb2 is not realized in healthy cells, or that additional regulatory interactions must be present, which are not captured in the current model. This result suggests that vessel progression may be thwarted by engineering feedback circuit fb2 to impose erratic motility in cells. Recent reports (e.g., Bashor et al., 2008; Scott and Pawson, 2009; Garrenton et al., 2009) demonstrate the capability of using engineered scaffold to reshape signaling pathways in yeast as well as mammalian cells, and construct synthetic positive- and negative-feedback loops. Conceivably, such technologies could be used to design fb2 for anti-angiogenesis therapeutic gains. We can perhaps reconcile the different relationships between Rac1 and RhoA found experimentally by pointing out that such studies look only at isolated systems, since it is not yet viable to monitor and measure the effect of single molecular perturbations on the entire signaling network. The utility of our computational model is that it captures a greater portion of the signaling network and can therefore aid in the interpretation of conflicting results, such as the relationship between Rac1 and RhoA, in the context of the larger system. Moreover, such a finding would necessitate a fundamental shift in how endothelial cell phenotypes have been represented in almost all mathematical models of angiogenesis.

3.4. Apoptosis response is more sensitive to noise suggesting a mechanism to induce anti-angiogenic effects

Another interesting question is how cells respond to a sudden, transient increase in stress (a "shock"). We model this by a sudden, complete randomization of internal molecular concentration levels, starting from a healthy cell that perceives both integrin and growth signal present, i.e., there is no external pressure to enter apoptosis. Fig. 6 details the results from our investigation. After a shock is applied, there is a transient increase in the probability of a peaked apoptotic response. The average height of the peak, as well as the time needed for the decrease of the apoptotic signal, increase with the noise rate p. If we interpret

p as the amount of stress already present in the system, where low p indicates a very healthy state (high reliability of signal processing) and high $p \sim 0.5$ an unhealthy state, then this observation implies that shocked cells are more likely to undergo programmed cell death the less healthy they are. Interestingly, to exploit this dependence biologically, the apoptotic switch must be slightly more sensitive compared to motility and growth signal switches in the sense that the cell's response should be triggered by a lower concentration of signaling molecules. For example, if the apoptotic response is triggered at a threshold of 0.47 (dashed line in Fig. 7, upper panel), compared to 0.5 for growth and motility, cells with $p > 0.15$ would generally undergo apoptosis, while cells with a smaller p value would not. The selective value of this property is immediately evident: it implements a dynamical mechanism that ensures that when the system is under stress or shocked, that regeneration occurs preferentially from the most healthy cells, while unhealthy cells are eliminated. Notice that a slight relative difference in equilibrium concentrations of signaling molecules involved in the respective cascades would have the same effect as a lowered threshold, which cannot be implemented in the current model since we normalize (maximal) concentrations. In principle, effects of this kind are experimentally testable in real organisms by comparing, e.g., the expression levels of the genes coding for signaling molecules involved in apoptosis and growth/motility, respectively. Manipulating the cell's apoptotic sensitivity could mediate pro- and anti-angiogenic effects and the results of such manipulations could be tested and quantified using this model and the experimental approaches suggested above.

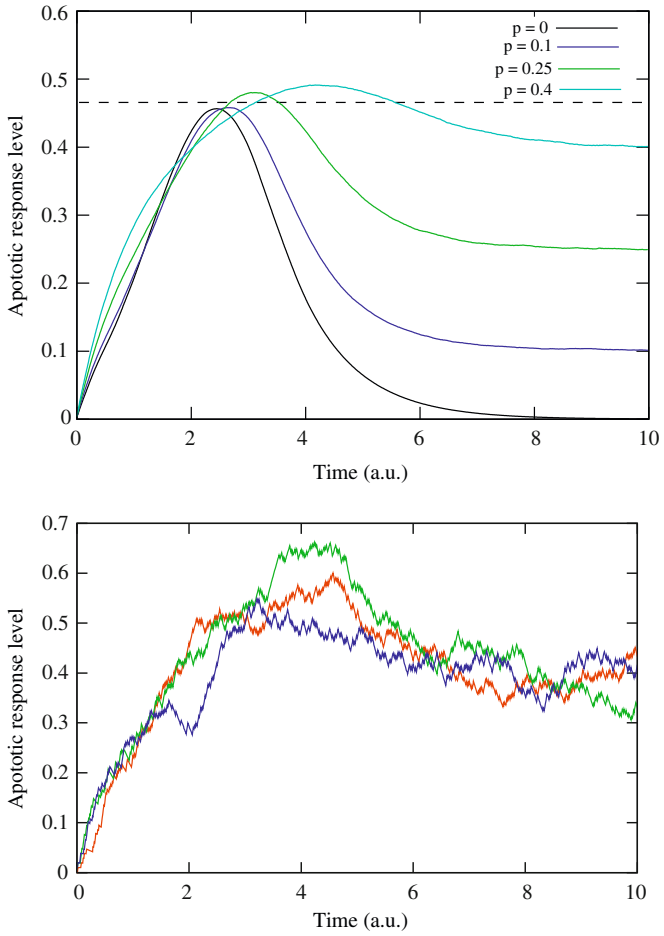

Fig. 7. Apoptosis regulation for anti-angiogenic effects. *Upper panel*: transient apoptotic signal for VEGF–RTK and ITG input with Rac1 activated. Curves averaged over 1000 different initial conditions of the internal network. The apoptosis signal increases as the noise level, p, increases, showing that the apoptosis response is sensitive to noise. This effect may have a biological function: when noise rates become to high, e.g., due to cell stress, apoptosis can be triggered before cells proliferate or move. This requires that the apoptotic switch is slightly more sensitive than the other switches, e.g., with a threshold of 0.47 (dashed line), any noise level $p > 0.15$ triggers apoptosis. *Lower panel*: transient apoptotic signal for three different initial internal states and different noise realizations, $p = 0.4$, to demonstrate the stochastic nature of the response.

3.5. *Inhibition studies suggest molecular targets for anti-angiogenic therapies*

Another utility of our model is that it can be employed as a therapeutic research tool to answer the question of whether targeted inhibition of specific signaling molecules will induce desired anti-angiogenic effects. Our Boolean network model allows systematic simulation and *in silico* statistical evaluation of protein inhibition. In these studies, a node in the signal transduction network is selected and set at a zero concentration level (corresponding to a Boolean off state). Signal transduction proceeds unimpeded in all other nodes. Table 2 summarizes the effects on cell phenotype of inhibiting all 19 possible single nodes. Inhibition of p53, PTEN or ROCK does not change the phenotype, i.e., these are neutral nodes and lead to the wildtype pattern as given in Fig. 3. Inhibiting Grb-2/Sos, Ras, PIP3, Rac, GSK-3β or FAK leads to apoptosis regardless of input signals, that is, given external cues that normally result in cell viability, apoptosis occurs when one of these six critical molecules is suppressed. We call these lethal phenotypes. At the network level, a clear pattern discerns neutral and lethal phenotypes. Neutral phenotypes are all found in the ECM integrin signaling cascade and may indicate redundant pathways parallel to the FAK–RhoA–Rac1–actin cascade. Whereas, Grb-2/Sos, Ras and FAK are located at the start of a signaling cascade and, as expected, induce a lethal phenotype when suppressed. Lethal phenotypes are, however, also produced by inhibition of PIP3, Rac1, GSK-3β or FAK, which are all central coordinators of cross-talk. This finding again highlights the crucial role of cross-talk for cell fate

Table 2
Phenotypic effects of single node inhibition. Phenotype vectors (middle column) contain the network response for all 16 possible configurations as shown in Fig. 3, using the following coding: 0=apoptosis, 1=proliferation, 2=motility, 3=proliferation+motility, 4=quiescence. The first 12 positions in the vector correspond to those configurations that lead to apoptosis in the wildtype (gray boxes in Fig. 3). The final four positions contain the responses when both VEGF-RTK and ITG signals are present and correspond to the rightmost column in Fig. 3, written from top to bottom.

Inhibited node	Phenotype vector	Phenotype
Grb-2/Sos	0000000000000000	Lethal
Ras	0000000000000000	Lethal
Raf-1	0000000000002322	
MEK 1	0000000000001144	
ERK 1/2	0000000000002222	
PI3K	0000000000004242	
PIP3	0000000000000000	Lethal
PKB/Akt	0000000000002322	
Rac1	0000000000000000	Lethal
GSK-3β	0000000000000000	Lethal
Bad	4123320000001342	Loss of regulation
β-catenin	0000000000001300	
FAK	0000000000000000	Lethal
p53	0000000000001342	Wildtype
PTEN	0000000000001342	Wildtype
RhoA	0000000000003322	
ROCK	0000000000001342	Wildtype
Actin	0000000000001144	
Cyclin D1	0000000000004242	

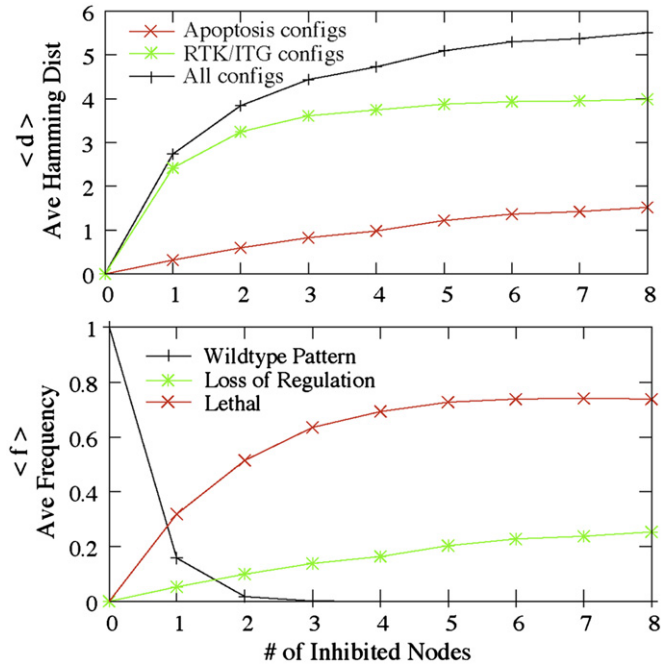

Fig. 8. Phenotypic effects of multiple node inhibition. (A) Average Hamming distance $<d>$ between mutants and wildtype phenotype as a function of the number of nodes that are inhibited. Black curve: average over all input configurations; Green curve: average only over configurations where both VEGF–RTK and ITG signals are present; Red curve: average over only those input configurations leading to apoptosis in the wildtype. (B) Average frequency $<f>$ of different phenotypes. Black curve: wildtype pattern; Red curve: lethal (always results in apoptosis regardless of input configuration); Green curve: loss of regulation and control (growth, motility, or quiescence replace apoptotic response in the wildtype). (For interpretation of the references to color in this figure legend, the reader is referred to the web version of this article.)

determination, and points to several key molecular targets that can be exploited for anti-angiogenesis interventions. Inhibition of nine other nodes (those unlabeled in column 3 of Table 2) maintain the wildtype apoptotic response when at least one external signal is missing, but lead to different phenotypes when both VEGF–RTK and ITG signals are present. An exception occurs with the inhibition of Bad, which leads to a "loss of regulation" phenotype, where instead of an appropriate apoptosis response, proliferative, motile, or quiescent phenotypes are expressed for 5 of the input configurations. This loss of control and ability to properly regulate apoptosis could explain hyperplasia and be used to promote angiogenesis, as is desired in wound healing for example.

A systematic study of multiple node inhibition strategies confirms this overall picture. Here we look at all possible inhibition combinations for up to eight nodes. For inhibition of a single node there are 19 possibilities, for two nodes there are 171 combinations, for three the number of possibilities increases to 969, etc., up to eight nodes and 50,388 possibilities. The general formula describing this combinatorial complexity is given by $k(k-1)/k!$, where k is the number of suppressed nodes. In this context, the Hamming distance $\langle d \rangle$ is the average number of input configurations – out of the 16 possible as shown in Fig. 3 – for which the network output differs from the wildtype vector (see Table 2). Fig. 8A shows the average Hamming distance between wildtype and mutant phenotype patterns as a function of number of nodes inhibited. A small value for $\langle d \rangle$ indicates that the network is close to a minimal essential network. In general, the Hamming distance increases only moderately with the number of inhibited nodes as shown by the black curve, which is an average over all possible input configurations. However, $\langle d \rangle$ is markedly different when we compare an average over only those configurations where both VEGF–RTK and ITG signals are present (green curve) to an average over only those input configurations leading to apoptosis in the wildtype (red curve). As the red curve in Fig. 8A shows, inhibition strategies result in only a small increase in the Hamming distance, indicating that apoptosis is a very tightly regulated and preserved phenotype. That is, molecular inhibition will not likely cause a deviation away from the states where apoptosis is expected, but it can and does cause once viable cell phenotypes to progress to apoptosis. Thus, molecular inhibition is a good strategy to achieve anti-angiogenic effects, but not pro-angiogenic effects. Interpreted from an evolutionary biology viewpoint, this means that when there are significant errors during signal transduction, cell death is the best response no matter what external signals the cell is receiving. On the other hand, the green curve in Fig. 8A shows that protein inhibition has a big impact on the wildtype phenotypes when both VEGF–RTK and ITG signals are present. Fig. 8B, which is a plot of frequency versus the number of inhibited nodes, shows that this increase in $\langle d \rangle$ is mainly due to the sharp increase in lethal phenotypes (red curve), where apoptosis occurs over 50% of the time given two suppressed nodes and roughly 75% of the time when there are four or more suppressed nodes. Loss of regulation phenotypes (green curve) increase in frequency to 25% and the wildtype pattern (black curve) is completely lost when three or more nodes are inhibited. The change in apoptotic response as a function of number of inhibited nodes is again a signature of robustness. When signaling pathways do not work reliably over time or become increasingly defective, the cell is programmed to commit suicide to promote the survival of the organism. This is the cell's first line of defense against disease. At the same time, however, the cell should be insensitive to intermittent internal fluctuations, as discussed for molecular noise in the previous sections. Our stochastic Boolean network model captures both of these phenomena. Looking again to Fig. 8B, the simultaneous increase in loss of regulation phenotypes indicates that these tasks are not always compatible and points to a possible conflict between the needs of reliability and responsiveness in cellular machinery.

An entire field of research is dedicated to the study of intracellular signaling cascades and biochemical reactions. A major contemporary challenge for experimental biologists and theoretical model builders is to unify this vast amount of information in a way that improves our understanding of the principal underpinnings driving angiogenic processes and that advances efforts aimed at the development of new therapies for treating cancer and other angiogenesis-dependent diseases. Discovering new therapeutic approaches to controlling angiogenesis hinges on the ability to integrate and interpret isolated data in the context of a molecular system of key signal transduction pathways, such as the one we propose here. Our novel Glass-type stochastic Boolean network model of signal transduction synthesizes a large body of compartmentalized research on angiogenesis-relevant molecular signaling pathways to increase our understanding of the molecular mechanisms associated with the regulation of cell growth, motility, quiescence, and apoptosis. Using this model, we propose molecular mechanisms that translate external signals to cell phenotype and suggest specific molecules and relationships that can be targeted for anti-angiogenesis cancer treatments. Further, this model framework provides us with the ability to hypothesize and test additional feedback circuits, perform knockout studies, and to predict the effects of receptor and pathway manipulation on system behavior and cell phenotype determination. Understanding how cell phenotype is controlled by multiple simultaneous external signals is a critical component to developing system level cancer treatment strategies. This model is a step in that direction.

Acknowledgements

This work was performed as part of the PhD dissertation research of ALB. ALB and YJ acknowledge support from the US Department of Energy under Contract no. DE-AC52-06NA25396. TLJ was supported in part by the Alfred P. Sloan Foundation and the James S. McDonnell Foundation.

References

Abedi, H., Zachary, I., 1995. Signaling mechanisms in the regulation of vascular cell migration. Cardiovasc. Res. 30, 544–556.
Albert, R., Othmer, H., 2003. The topology of the regulatory interactions predicts the expression pattern of the segment polarity genes in *Drosophila melanogaster*. J. Theor. Biol. 223, 1–18.
Amano, M., Ito, M., Kimura, K., Fukata, Y., Chihara, K., Nakano, T., Matsuura, Y., Kaibuchi, K., 1996. Phosphorylation and activation of myosin by Rho-associated kinase (Rho-kinase). J. Biol. Chem. 271, 20246–20249.
Bashor, C.J., Helman, N.C., Yan, S., Lim, W.A., 2008. Using engineered scaffold interactions to reshape MAP kinase pathway signaling dynamics. Science 319, 1539–1543.
Bauer, A.L., 2007. A multi-scale cell-based model to simulate and elucidate the mechanisms controlling tumor-induced angiogenesis. Ph.D. Dissertation, University of Michigan.
Bornholdt, S., Sneppen, K., 1998. Neutral mutations and punctuated equilibrium in evolving genetic networks. Phys. Rev. Lett. 81, 236–239.
Bornholdt, S., Rohlf, T., 2000. Topological evolution of dynamical networks: global criticality from local dynamics. Phys. Rev. Lett. 84, 6114–6117.
Chen, C.S., Mrksich, M., Huang, S., Whitesides, G.M., Ingber, D.E., 1998. Micropatterned surfaces for control of cell shape, position, and function. Biotechnol. Prog. 14, 356–363.
Corcoran, A., Del Maestro, R.F., 2003. Testing the "go or grow" hypothesis in human medulloblastoma cell lines in two and three dimensions. Neurosurgery 53, 174–184.
Cox, A.D., Der, C.J., 2003. The dark side of Ras, regulation of apoptosis. Oncogene 22, 8999–9006.
Datta, S.R., Brunet, A., Greenberg, M.E., 1999. Cellular survival: a play in three Akts. Genes Dev. 13, 2905–2927.
Derrida, B., Pomeau, Y., 1986. Random networks of automata: a simple annealed approximation. Europhys. Lett. 1, 45–49.
Eblen, S.T., Slack, J.K., Weber, M.J., Catling, A.D., 2002. Rac-PAK signaling stimulates extracellular signal-regulated kinase (ERK) activation by regulating formation of MEK1–ERK complexes. Mol. Cell. Biol. 22, 6023–6033.
Ferrara, N., Gerber, H., LeCouter, J., 2003. The biology of VEGF and its receptors. Nat. Med. 9, 669–676.
Folkman, J., 2006. Angiogenesis. Annu. Rev. Med. 57, 1–18.
Gagne, P., Akalu, A., Brooks, P.C., 2004. Challenges facing antiangiogenic therapy for cancer: impact of the tumor extracellular environment. Expert Rev. Anticancer Ther. 4, 129–140.
Garrenton, L.S., Braunwarth, A., Irniger, S., Hurt, E., Kunzler, M., Thorner, J., 2009. Nucleus-specific and cell cycle-regulated degradation of mitogen-activated protein kinase scaffold protein Ste5 contributes to the control of signaling competence. Mol. Cell. Biol. 29, 582–601.
Gerhardt, H., et al., 2003. VEGF guides angiogenic sprouting utilizing endothelial tip cell filopodia. J. Cell Biol. 161, 1163–1177.
Glass, L., 1973. The logical analysis of continous, non-linear biochemical control networks. J. Theor. Biol. 39, 103–129.
Glass, L., 1975. Combinatorial and topological methods in nonlinear chemical kinetics. J. Chem. Phys. 63, 1325–1335.
Gottardi, C.J., Wong, E., Gumbiner, B.M., 2001. E-cadherin suppresses cellular transformation by inhibiting β-catenin signalling in an adhesion-independent manner. J. Cell Biol. 153, 1049–1059.
Huang, S., Ingber, D.E., 1999. The structural and mechanical complexity of cell-growth control. Nat. Cell Biol. 1, E131–E138.
Hutchings, H., Ortega, N., Plouët, J., 2003. Extracellular matrix-bound vascular endothelial growth factor promotes endothelial cell adhesion, migration, and survival through integrin ligation. FASEB J. 17, 1520–1522.
Ishizaki, T., Naito, M., Fujisawa, K., Maekawa, M., Watanabe, N., Saito, Y., Narumiya, S., 1997. p160ROCK, a Rho-associated coiled-coil forming protein kinase, works downstream of Rho and induces focal adhesions. FEBS Lett. 404, 118–124.
Keely, P.J., Westwick, J.K., Whitehead, I.P., Der, C.J., Parise, L.V., 1997. Cdc42 and Rac1 induce integrin-mediated cell motility and invasiveness through PI(3)K. Nature 390, 632–636.
KEGG: Kyoto Encyclopedia of Genes and Genomes, 1995–2008.
Kauffman, S., 1969. Metabolic stability and epigenesis in randomly constructed genetic nets. J. Theor. Biol. 22, 437–467.
Kaufman, V., Mihaljev, T., Drossel, B., 2005. Scaling in critical random Boolean networks. Phys. Rev. E 72, 046124.
Klemm, K., Bornholdt, S., 2005. Stable and unstable attractors in Boolean networks. Phys. Rev. E 72, 055101(R).
Lampugnani, M.G., et al., 2003. Contact inhibition of VEGF-induced proliferation requires vascular endothelial cadherin, beta-catenin, and the phosphatase DEP-1/CD148. J. Cell Biol. 161, 793–804.
Leevers, S.J., Vanhaesebroeck, B., Waterfield, M.D., 1999. Signaling through phosphoinositide 3-kinases: the lipids take centre stage. Curr. Opin. Cell Biol. 11, 219–225.
Li, F., Long, T., Lu, Y., Quyang, Q., Tang, C., 2004. The yeast cell-cycle network is robustly designed. Proc. Natl. Acad. Sci. USA 101, 4781–4786.
Mantzaris, N.V., Webb, S., Othmer, H.G., 2004. Mathematical modeling of tumor-induced angiogenesis. J. Math. Biol. 49, 111–187.
Nobes, C.D., Hall, A., 1995. Rho, rac, and cdc42 GTPases regulate the assembly of multimolecular focal complexes associated with actin stress fibers, lamellipodia, and filopodia. Cell 18, 53–62.
Okumura, K., Mendoza, M., Bachoo, R.M., DePinho, R.A., Cavenee, W.K., Furnari, F.B., 1996. PCAF modulates PTEN activity. J. Biol. Chem. 281, 26562–26568.
Peixoto, T.P., Drossel, B., 2009. Noise in random Boolean networks. Phys. Rev. E 79, 036108.
Pollard, T.D., Borisy, G.G., 2003. Cellular motility driven by assembly and disassembly of actin filaments. Cell 112, 453–465.
Rohlf, T., 2008a. Critical line in random threshold networks with inhomogeneous thresholds. Phys. Rev. E 78, 066118.
Rohlf, T., 2008b. Self-organization of heterogeneous topology and symmetry breaking in networks with adaptive thresholds and rewiring. Europhys. Lett. 84, 10004.
Rohlf, T., Bornholdt, S., 2009. Morphogenesis by coupled regulatory networks: reliable control of positional information and proportion regulation. J. Theor. Biol. 261, 176–193.
Rubinfeld, B., Albert, I., Porfiri, E., et al., 1996. Binding of GSK-3B to the APC–B–catenin complex and regulation of complex assembly. Science 272, 1023–1026.
Ruoslahti, E., Reed, J.C., 1994. Anchorage dependence, integrins, and apoptosis. Cell 77, 477–478.
Somanath, P.R., Ciocea, A., Byzova, T.V., 2009. Integrin and growth factor receptor alliance in angiogenesis. Cell Biochem. Biophys. 53 (2), 53–64.
Schoenwaelder, S.M., Burridge, K., 1999. Bidirectional signaling between the cytoskeleton and integrins. Curr. Opin. Cell Biol. 11, 274–286.
Scott, J.D., Pawson, T., 2009. Cell signaling in space and time: where proteins come together and when they're apart. Science 326, 1220–1224.
Sephel, G.C., Kennedy, R., Kudravi, S., 1996. Expression of capillary basement membrane components during sequential phases of wound angiogenesis. Matrix Biol. 15, 263–279.
STKE: The signal transduction knowledge environment. Science Database of Cell Signaling.
Solé, R., Luque, B., 1995. Phase transitions and antichaos in generalized Kauffman networks. Phys. Lett. A 196, 331–334.
Song Li, S.A., Albert, R., 2006. Predicting essential components of signal transduction networks: a dynamic model of guard cell abscisic acid signaling. PLoS Biol. 4, 1732–1748.
Stromblad, S., Becker, J.C., Yebra, M., Brooks, P.C., Cheresh, D.A., 1996. Suppression of p53 activity and p21WAF1/CIP1 expression by vascular cell integrin alpha v beta3 during angiogenesis. J. Clin. Invest. 98, 426–433.
Thomas, R., 1973. Boolean formalization of genetic control circuits. J. Theor. Biol. 42, 563–585.
Yancopoulos, G.D., Davis, S., Gale, N.W., Rudge, J.S., Wiegand, S.J., Holash, J., 2000. Vascular-specific growth factors and blood vessel formation. Nature 407, 242–248.
Zanetti, A., Lampugnani, M.G., Balconi, G., Breviario, F., Corada, M., Lanfrancone, L., Dejana, E., 2002. Vascular endothelial growth factor induces Shc association with vascular endothelial cadherin: a potential feedback mechanism to control vascular endothelial growth factor receptor-2 signaling. Arterioscler. Thromb. Vasc. Biol. 22, 617–622.